Electrochemical and Solid-State Letters, **11** (3) H51-H54 (2008)
1099-0062/2007/11(3)/H51/4/$23.00 © The Electrochemical Society

Bulk-Limited Current Conduction in Amorphous InGaZnO Thin Films

Hyun-Joong Chung, Jong Han Jeong, Tae Kyung Ahn, Hun Jung Lee, Minkyu Kim, Kyungjin Jun, Jin-Seong Park, Jae Kyeong Jeong,[z] Yeon-Gon Mo, and Hye Dong Kim

Samsung SDI Company, Limited, Corporate Research and Development Center, 428-5, Gongse-Dong, Kiheung-gu, Yongin-si, Gyeonggi-do 449-902, Korea

The current conduction mechanism in radio frequency sputtered amorphous indium gallium zinc oxide (a-IGZO) films was investigated using model devices designed to mimic the carrier injection from an electrode to an a-IGZO channel in thin-film transistors. Interface-limited mechanisms, such as thermionic emission and Fowler–Nordheim tunneling, clearly fail to fit the current–voltage (*I-V*) curves. Instead, the *I-V* characteristics of the a-IGZO devices fit well within the framework of space-charge-limited current, whereas the conduction is enhanced by the Frenkel effect at high field (>0.1 MV/cm).
© 2007 The Electrochemical Society. [DOI: 10.1149/1.2826332] All rights reserved.

Manuscript submitted November 15, 2007; revised manuscript received November 28, 2007.
Available electronically December 26, 2007.

ZnO-based semiconductors have recently attracted a tremendous amount of attention due to their high optical transparency and tunable electrical conductivity, which enables the fabrication of novel electronic devices such as UV light-emitting devices and transparent thin-film transistors (TFTs).[1] Among the various ZnO-based semiconductor materials, amorphous In–Ga–Zn oxide (a-IGZO) is of particular interest for the fabrication of high-performance TFTs[2-5] and more interestingly, the prototypes of active-matrix liquid crystal displays[6] and organic light-emitting devices (AMOLEDs).[7-9] In addition to their transparency, a-IGZO TFTs have unique advantages that allow them to replace polycrystalline-Si (p-Si) TFTs for AMOLEDs. For example, a-IGZO TFTs are free from the nonuniformity of the mobility and threshold voltage that stems from the grain boundaries of p-Si TFTs because of their amorphous nature. Their large charge carrier mobility ($>10\ cm^2/V\ s$) and excellent subthreshold gate swing (0.20 V/dec) are sufficient to drive large-area AMOLEDs. Moreover, the large-area deposition of uniform thin films of a-IGZO can be accomplished at low temperature by physical vapor deposition techniques, thereby enabling the mass production of AMOLEDs on flexible plastic substrates or cheap soda-lime glasses.[2]

In our earlier reports, inverted staggered a-IGZO TFTs were shown to be contact-limited at short channel lengths.[5,10] The contact resistance R_C can be extracted by a transmission line method (TLM), which involves plotting the transistor on-resistance, R_T, as a function of channel length L according to the following equation

$$R_T(L) = \frac{L}{\mu_{eff} W C_i (V_G - V_T)} + R_C \qquad [1]$$

where μ_{eff}, W, C_i, V_G, and V_T are effective mobility at the channel region, channel width, gate dielectric capacitance, gate and threshold voltages, respectively.[11] Figure 1 shows a typical example of a TLM plot of a-IGZO TFTs, where the extracted $R_C\ W$ is $\sim 200\ \Omega$ cm. The typical $R_C W$ values are ~ 1 and $>1000\ \Omega$ cm for p-Si and organic TFTs, respectively.[10,12] In addition, Ar plasma treatment of the electrode/a-IGZO contact improves the field-effect mobility and subthreshold gate swing from $3.3\ cm^2/Vs$ and 0.23 V/dec to $9.1\ cm^2/Vs$ and 0.19 V/dec, respectively.[13] Given that the contact resistance in the inverted staggered TFT is the summation of the voltage drop at the electrode/a-IGZO interface and in the a-IGZO bulk, which is located in the overlap region of the source electrode and gate metal, a natural question arises: Which mechanism limits the current conduction in a-IGZO TFTs?

In this article, we show that the large contact resistance originates from the bulk a-IGZO itself rather than from the interface between the source/drain electrode and the a-IGZO by investigating the current conduction mechanism of the device structure of the electrode/a-IGZO/electrode. Specifically, the current–voltage (*I-V*) characteristics of the a-IGZO devices fit well within the framework of the space-charge-limited current (SCLC) mechanism, where the conduction is enhanced by the Frenkel effect when a high electric field is applied (>0.1 MV/cm). Interface-limited mechanisms, such as Richardson–Schottky (R-S) thermionic emission and Fowler–Nordheim (F-N) tunneling, clearly fail to fit the *I-V* curve.

Experimental

MoW sputtered on a SiO_2/glass substrate with a surface area of 50×50 mm was used as the bottom electrode. The a-IGZO film with a thickness of 50 nm was grown by radio frequency (rf) sputtering on the bottom electrode at room temperature. The sputtering was carried out at a gas mixture ratio of $Ar/O_2 = 65{:}35$ and an input rf power of 450 W. Inductively coupled plasma mass spectrometry showed that the atomic ratio of the a-IGZO film was In/Ga/Zn = 2.2:2.2:1.0. Indium zinc oxide (IZO) top electrodes (200 nm thick; circular with 200 μm diameter) were formed by sputtering in the same chamber at room temperature. A shadow metal mask was used to pattern the top electrode. The resistivity of deposited IZO was $8 \times 10^{-4}\ \Omega$ cm, measured by four-point probe. Because semiconducting a-IGZO has a carrier concentration of less than $10^{18}/cm^3$

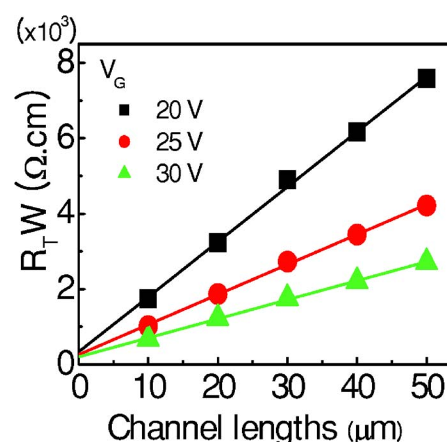

Figure 1. (Color online) The transistor on resistance $R_T W$ as a function of L at $V_{DS} = 5.1$ V for the a-IGZO TFTs. Extracted contact resistance $R_{SD} W$ is 200 Ω cm.

[z] E-mail: jaekyeong.jeong@samsung.com

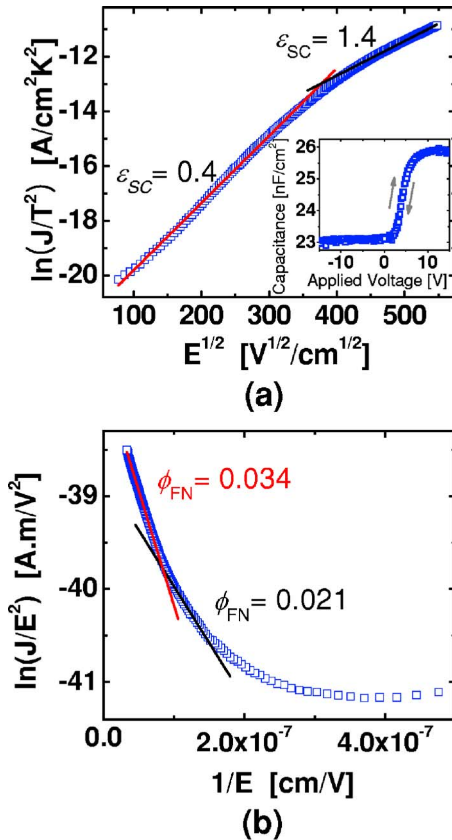

Figure 2. (Color online) (a) R-S and (b) F-N plots of the a-IGZO films at 298 K. ε_{SC} and $\phi_{F\text{-}N}$ denote the dielectric constant of a-IGZO and the electrode/a-IGZO potential barrier height for tunneling, respectively, fitted from the graphs. The unphysical ε_{SC} and $\phi_{F\text{-}N}$ values clearly indicate that R-S and F-N mechanisms fail to predict the current conduction. (Inset) High-frequency (100 kHz) *C-V* curves of the IZO/a-IGZO (50 nm)/SiN_x/MoW at 298 K, where an ε_s value of 11.5 is extracted. Arrows indicate voltage sweep direction.

and its mobility is ~ 10 cm^2/V s,[1] the resistivity of our IZO electrode was at least three orders smaller than that of a-IGZO. Thus, the voltage drop within IZO electrode was negligible. Finally, the samples were annealed at 350°C for 1 h in an N_2 atmosphere. The *I-V* characteristics of the samples were measured with an Agilent 4156C precision semiconductor parameter analyzer. A positive voltage sweep was applied to the bottom electrode, while the top electrode was grounded to mimic the situation of carrier injection from the source to the channel in a driving TFT. Delay times ranging from 0.1 to 2 s were tested for the *I-V* measurements. The delay time did not significantly change the *I-V* curve. The three temperatures, 298, 323, and 348 K, were used to observe the temperature dependence in current conduction.

Results and Discussion

To prove that the current conduction was not limited by the injection at the electrode/a-IGZO interface, the *I-V* data at 298 K were fitted with the R-S and F-N equations in Fig. 2a and b, respectively. The R-S model postulates that the conduction is limited by thermionic injection at the interface and the current density, *J*, can be expressed as

$$J \propto T^2 \exp\left(-\frac{\phi_0}{kT}\right)\exp\left(\left(\frac{q}{4\pi\varepsilon_0\varepsilon_{SC}}\right)^{1/2}\frac{E^{1/2}}{kT}\right) \quad [2]$$

where T, ϕ_0, k, q, ε_0, ε_{SC}, and E are the absolute temperature, barrier height, Boltzmann's constant, electron charge, the permittivity of vacuum, the dielectric constant of a-IGZO obtained by the R-S model, and applied electric field, respectively.[14] Therefore, the validity of the R-S mechanism for a given *I-V* measurement can be tested by comparing the value of ε_{SC} obtained from the slope of the plot of $\ln(J/T^2)$ vs $E^{1/2}$ to the known high-frequency dielectric constant of a-IGZO, ε_s.[15,16] An ε_s value of 11.5 was experimentally obtained by comparing the accumulation and depletion capacitances of the high-frequency (100 KHz) capacitance–voltage *C-V* curves of the IZO/a-IGZO/SiN_x/MoW samples at 298 K (inset of Fig. 2a). Fitting the slopes of Fig. 2a gives ε_{SC} values of 0.4 and 1.4 at $15 < E < 120$ and $175 < E < 300$ kV/cm, respectively, both of which are physically unacceptable. Thus, the R-S mechanism is not a controlling factor that limits the current conduction in this system.

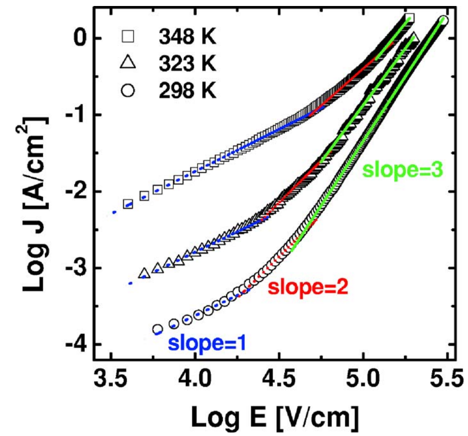

Figure 3. (Color online) Log *J* vs log *E* plots of the a-IGZO films. Lines and slopes are guides to the eye. See text for details.

Another possible interface-limited conduction mechanism is field emission, i.e., E-field assisted tunneling. By postulating that the barrier has a triangular shape, the F-N model predicts the current density to be

$$J \propto E^2 \exp\left[-\frac{4\pi(2m^*)^{1/2}}{h}\frac{2\phi_{F\text{-}N}^{3/2}}{3qE}\right] \quad [3]$$

where m^*, h, and $\phi_{F\text{-}N}$ are the effective mass of the charge carrier, Planck's constant, and the barrier height obtained by the F-N model, respectively.[17] The slopes of the plot of $\ln(J/E^2)$ vs $(1/E)$ in Fig. 2b show $\phi_{F\text{-}N}$ values of less than 0.04 eV in all the ranges, which is comparable to the kT value of 0.026 eV at 25°C. Therefore, the F-N mechanism can also be ruled out.

To examine the validity of the SCLC mechanism, Fig. 3 shows the plots of $\log(J)$ vs $\log(E)$ taken in the temperature range between 298 and 348 K. Linear fittings to the log–log plot reveal a power-law dependence on the current flow at a given electric field. Within the framework of the SCLC mechanism, the plots are linearly fitted and the power n indicates the conduction mechanism at a given electric field E. At all temperatures, the $\log(J)$–$\log(E)$ plot undergoes a transition from linear, to quadratic, to cubic power law scaling behavior as E increases, as summarized in Table I. This is in qualitative agreement with the theoretical expectation of SCLC with shallow traps, where a transition from linear ($J \propto E$), to Mott–Gurney's law ($J \propto E^2$) to a trap-related high-field effect ($n > 2$) is expected with increasing E.[18,19]

The origin of the linear *J-E* region has been attributed to Ohm's law[17] or a Schottky-limited current.[16,18,19] The former case may arise at low applied voltages, where the density of thermally generated free carriers in the bulk a-IGZO, N_e, is predominant over the injected carrier by the external field.[17,a] In this case the

[a] In this part, the terminology "thermally generated" does not refer to the leakage current.

Table I. Summary of fitting results from Fig. 3 and 4.[a]

	SCLC fittings						Frenkel effect			
	Linear *J-E*		Mott–Gurney		Trap-assisted		SCL + F		Poole–Frenkel	
Temperature (K)	E	n	E	n	E	n	E	ε_{SCL+F}	E	$\varepsilon_{P\text{-}F}$
298	$E < 20$	1.06	$20 < E < 40$	2.18	$E > 40$	3.37	$40 < E < 180$	9.2	$E > 190$	12.4
323	$E < 25$	1.06	$25 < E < 75$	2.18	$E > 75$	2.96	-	-	$E > 155$	11.5
348	$E < 45$	1.10	$45 < E < 150$	1.94	$E > 150$	2.69	-	-	$E > 100$	10.3

[a] The unit of E is kV/cm.

electric field where the *J-E* scaling relation transits from linear to square E_{tr} scales with $E_{tr} \propto N_e/\varepsilon_s$.[17] The latter mechanism is valid when the mean free path of the charge carriers injected from the electrode is less than the width of the Schottky barrier and $E_{tr} = [1/\mu(T)]\sqrt{(kT/2\pi m^*)}$, where $\mu(T)$ is the carrier mobility.[19] The latter mechanism has been shown to be valid for bulk-limited current cases.[16,18] From Table I, the observed value of E_{tr} increases by about a factor of 2 when T increases from 298 to 348 K. For semiconducting IGZO, Hall measurements have shown that both N_e and $\mu(T)$ significantly increase with increasing temperature and are roughly proportional to $\exp(-1/T)$.[20] Therefore, the twofold increase in E_{tr} can be attributed to the increase in N_e with increasing temperature and, thus, the linear *J-E* current behavior can be attributed to ohmic current in our system.

With the presence of a strong E, charge transport can be enhanced by the Frenkel effect, which is a lowering of the potential barrier for a charge carrier escaping from a trap by an electric field.[17,21] The Frenkel effect can enhance the space-charge current, leading to a deviation from Mott–Gurney's law at a high electric field. With the abundance of deep traps and at a higher electric field, the thermal excitation of the charge carriers at deep traps can dominate the current flow due to the lowering of the potential barrier. The former mechanism was suggested by Murgatroyd (SCL + F) and can be expressed as[21]

$$J \propto E^2 \exp\left[\frac{0.891}{kT}\left(\frac{q^3V}{\pi\varepsilon_0\varepsilon_{SCL+F}d}\right)^{1/2}\right] \quad [4]$$

and the $\ln(J/E^2)$ vs $E^{1/2}$ plot at 298 K is shown in Fig. 4a. The latter is called the Poole–Frenkel (P-F) detrapping model and is expressed as

$$J \propto E \exp\left(-\frac{\phi_{P\text{-}F}}{kT}\right)\exp\left[\left(\frac{q}{\pi\varepsilon_0\varepsilon_{P\text{-}F}}\right)^{1/2}\frac{E^{1/2}}{kT}\right] \quad [5]$$

where $\phi_{P\text{-}F}$ is the barrier height of a trap before its lowering.[17] Figure 4b shows the plot of $\ln(J/E)$ vs $E^{1/2}$. From the plots and model fittings in Fig. 4a and b, the fitted ε_{SCL+F} and $\varepsilon_{P\text{-}F}$ values are in good agreement with ε_s at $40 < E < 180$ and Fig. 3b at $E > 190$ kV/cm, respectively. Therefore, one can conclude that the charge transport is governed by the SCLC mechanisms (linear *J-V* behavior followed by Mott–Gurney's square law) and the Frenkel effect becomes important at a high electric field (SCL + F and P-F). Table I summarizes the variation of the dominating charge-transport mechanism with the temperature and electric field.

The effect of temperature on the P-F current is shown in the inset of Fig. 4b. From the linear fitting of the $\ln(J/E)$ vs $E^{1/2}$ plots, $\varepsilon_{P\text{-}F}$ is found to decrease monotonically from 12.4 to 10.3 as the temperature increases from 298 to 348 K. The reduction of the high-frequency dielectric constant with increasing temperature is in qualitative agreement with an earlier study of rf-sputtered ZnO films.[22] The $\phi_{P\text{-}F}$ value can be calculated from the relation $\phi_{P\text{-}F} = -kG + \sqrt{(qE/\pi\varepsilon_0\varepsilon_{P\text{-}F})}$, where G is the slope of the $\ln(J/E)$ vs $(1/T)$ plot. By plotting the $\ln(J/E)$ values at 200 kV/cm, $\phi_{P\text{-}F}$ is found to be 0.35 eV. The current conduction of rf-sputtered amorphous silicon carbide[15] and silicon monoxide[17] is governed by the P-F mechanism when E is of the order of 10^2 kV/cm and the $\phi_{P\text{-}F}$ values are ca. 0.35 eV. Thus, one can conjecture that the abundance of traps at a depth of 0.35 eV can cause the P-F mechanism to dominate when the current flow is bulk-limited.

Conclusion

In summary, the current injection from the source/drain electrode to the channel in a-IGZO TFTs is bulk-limited rather than interface-limited. Specifically, the conduction is governed by the SCL mechanism at a low electric field. At a high field, thermionic injection of the charge carriers from the traps becomes important, leading to the

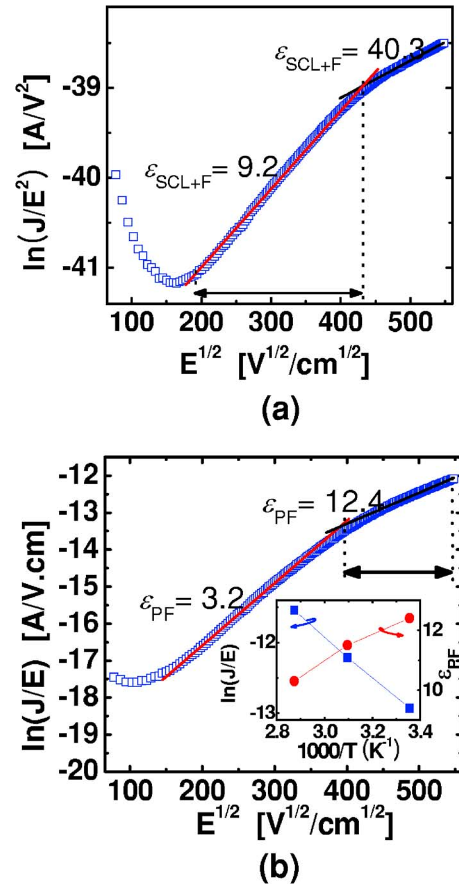

Figure 4. (Color online) (a) Murgatroyd (SCL + F) and (b) P-F plots at 298 K. Shaded regions indicate the electric field with good fitting, where each mechanism is dominant for current conduction. The inset in (b) shows the temperature dependence on the P-F current at 200 kV/cm and fitted dielectric constant, $\varepsilon_{P\text{-}F}$.

enhancement of the current flow by the SCL + F and P-F mechanisms. It is notable that hopping was found to be the dominant conduction mechanism in numerous studies of single- or polycrystalline $InGaO_3(ZnO)_5$[21] and polycrystalline ZnO[22,23] films. We believe that this discrepancy arises from the amorphous nature of our system. Conclusively, our results suggest that the reduction of the R_{SD} value required to fabricate high-performance, short-channel (<10 μm) TFTs can be achieved by tuning the bulk property of the a-GIZO film. We hope that this study will aid researchers to optimize the performance of a-IGZO-based TFTs.

Samsung SDI Company, Limited, assisted in meeting the publication costs of this article.

References

1. H. Hosono, *J. Non-Cryst. Solids*, **352**, 851 (2006).
2. K. Nomura, H. Ohta, A. Takagi, T. Kamiya, M. Hirano, and H. Hosono, *Nature (London)*, **432**, 488 (2004).
3. H. Yabuta, M. Sano, K. Abe, T. Aiba, T. Den, H. Kumomi, K. Nomura, T. Kamiya, and H. Hosono, *Appl. Phys. Lett.*, **89**, 112123 (2006).
4. D. Kang, H. Lim, C. Kim, I. Song, J. Park, Y. Park, and J. Chung, *Appl. Phys. Lett.*, **90**, 192101 (2007).
5. M. Kim, J. H. Jeong, H. J. Lee, T. K. Ahn, H. S. Shin, J.-S. Park, J. K. Jeong, Y.-G. Mo, and H. D. Kim, *Appl. Phys. Lett.*, **90**, 212114 (2007).
6. T. Hirao, M. Furuta, H. Furuta, T. Matsuda, T. Hiramatsu, H. Hokari, and M. Yoshida, in *Proceedings of SID Digest*, **37**, 18 (2006).
7. H. N. Lee, J. W. Kyung, S. K. Kang, D. Y. Kim, M. C. Sung, S. J. Kim, C. N. Kim, H. G. Kim, and S. T. Kim, in *Proceedings of IDW*, pp. 663–666 (2007).
8. S. K. Park, C.-S. Hwang, J.-I. Lee, S. M. Chung, Y. S. Yang, L.-M. Do, and H. Y. Chu, in *Proceedings of SID Digest*, **13**, 25 (2006).
9. J. K. Jeong, M. Kim, J. H. Jeong, H. J. Lee, T. K. Ahn, H. S. Shin, K. Y. Kang, H. Seo, J. S. Park, H. Yang, et al., in *Proceedings of IMID*, pp. 145–148 (2007).
10. J. S. Park, J. K. Jeong, Y.-G. Mo, H. D. Kim, and S.-I. Kim, *Appl. Phys. Lett.*, **90**, 262106 (2007).
11. D. K. Schroder, *Semiconductor Material and Device Characterization*, 3rd ed., Chap. 4, p. 208, Wiley, Hoboken, NJ (2006).
12. A. Valletta, L. Mariucci, G. Fortunato, and S. D. Brotherton, *Appl. Phys. Lett.*, **82**, 3119 (2003).
13. G. Horowitz, P. Lang, M. Mottaghi, and H. Aubin, *Adv. Funct. Mater.*, **14**, 1069 (2004).
14. Y. Kim, S. Ohmi, K. Tsutsui, and H. Iwai, *Jpn. J. Appl. Phys., Part 1*, **44**, 4032 (2005).
15. W. K. Choi, L. J. Han, and F. L. Loo, *J. Appl. Phys.*, **81**, 276 (1997).
16. C. S. Hwang, *J. Mater. Res.*, **16**, 3476 (2001).
17. K. C. Kao and W. Hwang, *Electrical Transport in Solids*, Chaps. 2, 3, and 5, Pergamon, New York (1981).
18. F. D. Morrison, P. Zubko, D. J. Jung, J. F. Scott, P. Baxter, M. M. Saad, R. M. Bowman, and J. M. Gregg, *Appl. Phys. Lett.*, **86**, 152903 (2005).
19. J. G. Simmons, *Phys. Rev. Lett.*, **15**, 967 (1965).
20. K. Nomura, T. Kamiya, H. Ohta, K. Ueda, M. Hirano, and H. Hosono, *Appl. Phys. Lett.*, **85**, 1993 (2004).
21. P. N. Murgatroyd, *J. Phys. D*, **3**, 151 (1970).
22. V. Gupta and A. Mansingh, *Phys. Rev. B*, **49**, 1989 (1994).
23. K. Eda, *J. Appl. Phys.*, **49**, 2964 (1978).